Industry Science and Engineering Vol. 2 No. 11, 2025

Investigation into the Preload Application Behavior of Grooved Rivet Connections

Tao Yu, Shuai Dong*, Xu He, Qi Li, Xiaolian Zhang
Meishan CRRC Fastening System Co., Ltd., Meishan, Sichuan, China
**Corresponding Author*

Abstract: Ring-grooved rivets, as a type of special fastener, play a critical role in wind power equipment structures, where their connection reliability directly affects the structural integrity of key components such as wind turbine towers, nacelles, and blade connections. To investigate the preload formation mechanism of high-strength ring-grooved rivets used in wind power applications, this paper systematically analyzes the stress state of the bushing during the installation process. Finite element analysis software was employed to conduct numerical simulations of the bushing forming behavior, stress distribution characteristics in the rivet groove region, and material flow patterns during the riveting process. Preload detection tests were carried out under different displacement lengths using a smart displacement-controlled pump station. The results indicate that the preload of wind power ring-grooved rivets originates from the multi-stage locking effect formed by the progressive filling of the bushing material into the rivet grooves under axial compression, with the final preload being the cumulative result of the compressive forces at each stage. This study can provide a theoretical basis and reference for the engineering application and process optimization of ring-grooved rivets in the wind power sector.

Keywords: Ring-Grooved Rivet; Wind Power Equipment; Preload; Finite Element Simulation; Bushing Forming; Multi-Stage Locking Effect

1. Introduction

Grooved rivets, as high-performance fasteners based on the principle of plastic deformation, are widely used in critical connection areas of wind power equipment such as tower flange connections, nacelle bases, and blade bearings. Their connection reliability is directly related to the structural safety and service life of the unit. Unlike traditional threaded connections that rely on friction to transfer loads, grooved rivets form a permanent mechanical interlock by axially stretching the collar to cause plastic deformation and embed it into the locking groove. Preload, as the core factor ensuring connection reliability, directly determines the anti-loosening performance and long-term stability of the joint through its loading characteristics. However, the formation mechanism, evolution law, and the influence of key process parameters on the preload during the riveting process of grooved rivet connections remain unclear, which limits the precise control and optimized application of this connection technology in engineering. Currently, many scholars have conducted research on grooved rivets and related fastening connection technologies. Zhang Tianxiong et al. [1] conducted mechanical performance tests on high-strength stainless steel short-tail grooved rivets, revealing their load-bearing capacity under static loads, but did not systematically analyze the formation process of preload. Zhang Qin et al. [2] used Deform software to numerically simulate the forming process of grooved rivets, analyzing the metal flow behavior of the collar, but the study on the dynamic loading behavior of preload was insufficient. Li Wenchao et al. [3] studied the interference fit riveting process based on DEFORM-3D, emphasizing the influence of process parameters on connection quality, but did not establish a quantitative relationship between parameters and preload. Chen Weijing [4] systematically analyzed the loosening mechanism and anti-loosening techniques of threaded connections, providing a comparative basis for the anti-loosening advantages of grooved rivets, but did not involve preload loading characteristics. Li Jin et al. [5] proposed a strength modeling method for riveted forming

connection structures, but there are still modeling blind spots in the quantitative control of preload. Zuo Shibin et al. [6] explored an ultrasonic detection method for clamping force based on the acoustoelastic principle, providing a new idea for the non-destructive detection of preload in grooved rivets, but did not involve the mechanism study of the loading process. Furthermore, Li Huixun et al. [7] used ANSYS to simulate bolt preload, providing a methodological reference for the numerical simulation of preload, but their research object did not cover the special structure of grooved rivets. Zhou Kun et al. [8] analyzed the calculation and control of preload in flange bolt connections, but the applicability of their conclusions to the grooved rivet system needs verification. Qian Jin et al. [9] conducted high-fidelity simulation and experimental verification of bolt preload under tightening torque, improving the prediction accuracy of preload, but their model did not consider the unique plastic forming mechanism of grooved rivets. Huang Jiawei [10] analyzed the strength of bolted connections through orthogonal experiments, providing a way for parameter optimization, but did not deeply explore preload loading characteristics. Dai Runda et al. [11] conducted group riveting tests on the corrosion resistance and clamping force of grooved rivet connections, revealing the influence of environmental factors on connection performance, but the research on the formation mechanism of preload was insufficient. Wang Wen et al. [12] studied the corresponding relationship between blade load and bolt preload, providing a reference for the correlation analysis between external load and preload, but did not involve the connection characteristics of grooved rivets. Although the aforementioned research has made some progress in the connection mechanism, process simulation, detection methods, and preload control of grooved rivets, the following research gaps still exist: (1) Lack of systematic research on the dynamic evolution law of preload during the riveting process of grooved rivet connections; (2) The existing numerical models have insufficient capability to characterize the formation mechanism of preload under the unique forming process of grooved rivets; (3) The influence mechanism of key process parameters on preload loading characteristics is not yet clear, lacking a theoretical basis for process optimization. Therefore, based on a combination of finite element simulation and experimental verification, this paper systematically studies the preload loading characteristics of grooved rivet connections during the riveting process, reveals the formation mechanism and dynamic evolution law of preload, in order to provide theoretical support and experimental basis for the precise control and performance optimization of grooved rivet connection processes.

2. Connection Principle and Mechanical Analysis of the Installation Process for Grooved Rivets

The grooved rivet assembly primarily consists of the grooved rivet and the locking collar, with its installation tool comprising key components such as the anvil and jaws. The overall structure is illustrated in Figure 1. The installation process, depicted in Figure 2, is as follows: First, the rivet is passed through the wind power structural components to be connected (e.g., a tower flange), and the locking collar is screwed onto the opposite side. Subsequently, the tail shank of the rivet is engaged into the jaws of the installation tool. Upon activation of the equipment, the anvil moves axially downwards. After contacting the end face of the locking collar, it applies a continuous axial pressure. Under this pressure, the locking collar undergoes plastic deformation, and its internal metal is forced to flow radially, gradually filling the annular locking grooves on the rivet shank, thereby forming a mechanical interlock. The installation stroke is considered complete when the lower end face of the anvil makes full contact with the flange face of the locking collar. Following this, the anvil retracts, and the riveting process is finished.

To deeply analyze the deformation mechanism of the locking collar and the formation of preload, Figure 3 (a) and (b) provide a mechanical breakdown of the intermediate installation stage. As shown in Figure 3 (a), when the anvil descends to a specific position, its inner wall contacts the outer surface of the locking collar at point a. At this stage, the locking collar is subjected to a concentrated force F applied by the anvil; its force state is illustrated in Figure 3 (b). This applied force F can be resolved into a radial component F_1 and an axial component F_2. The radial component F_1

is the key load driving the radial plastic flow of the locking collar metal into the rivet's grooves. Conversely, the axial component F_2 promotes the axial flow of part of the locking collar metal along the rivet shank. Under the synergistic action of these two components, the collar material is progressively extruded into each successive groove, ultimately completing the formation of the entire locking structure. This multi-stage locking mechanism, established through metal plastic flow, is the fundamental reason why grooved rivets achieve high preload and possess excellent anti-loosening and fatigue resistance properties. To precisely reveal the flow patterns of the collar material, stress distribution, and the dynamic generation mechanism of the preload during this process, the subsequent section will employ Deform software for a finite element numerical simulation of this riveting process.

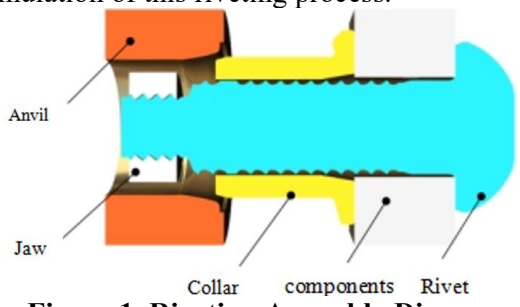

Figure 1. Riveting Assembly Diagram

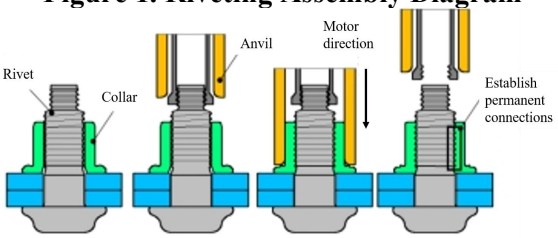

Figure 2. Installation Schematic Diagram

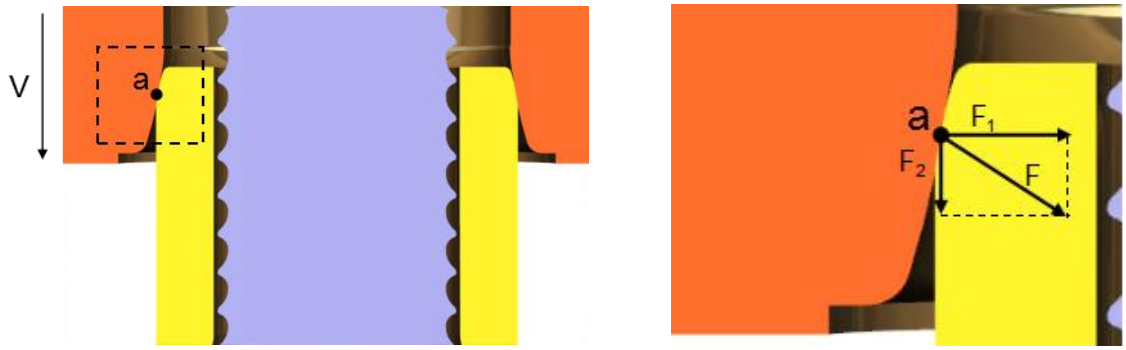

(a) Schematic Diagram of Anvil Movement **(b) Enlarged Partial View**

Figure 3. Force Analysis

3. Finite Element Modeling and Mechanism Analysis of the Grooved Rivet Installation Process

To systematically reveal the formation mechanism of the preload and the plastic flow behavior of the locking collar during the installation of grooved rivets, this section establishes a complete finite element model of the riveting process based on the DEFORM-3D platform. Using numerical simulation methods, it focuses on analyzing the stress evolution and material flow characteristics during the engagement process between the locking collar and the rivet grooves, providing theoretical support for the anti-loosening and fatigue-resistant design of grooved rivets in wind power structures.

3.1 Finite Element Modeling and Parameter Setting

Given the limitations of DEFORM software in the direct modeling of complex assemblies, this study used UG NX software to create a complete three-dimensional assembly model comprising the grooved rivet, locking collar, connected plates, jaws, and anvil (Figure 4). Each component was imported into DEFORM in STL format for pre-processing. To improve computational efficiency and focus on the core contact area between the locking collar and the rivet grooves, the model was reasonably simplified: the jaws and anvil were treated as rigid bodies, and their non-critical geometric features were omitted, the material parameters are listed in Table 1.

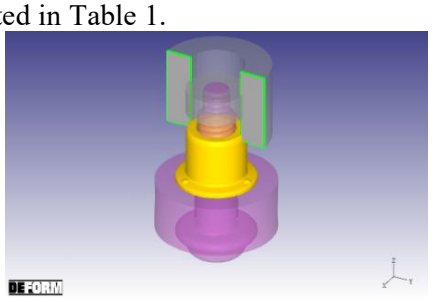

Figure 4. Rivet Installation Assembly Diagram

Table 1. Material Properties of Each Component

Grooved Rivet Component	Material	Elastic Modulus/GPa	Poisson's Ratio
Rivet	Alloy Steel	210	0.3
Collar	Low Carbon Steel	210	0.3
Connected Plates	Alloy Steel	210	0.3

3.2 Results Analysis and Discussion

Key mechanical responses throughout the entire riveting process were obtained through finite element solution. As shown in Figure 5 (a), a designed clearance exists between the inner wall of the locking collar and the rivet grooves before installation. The stress distribution within the assembly is uniform and close to zero, consistent with the mechanical characteristics of the initial installation stage. As shown in Figure 5 (b), after the rivet installation is completed, the metal from the inner wall of the locking collar fills all seven grooves on the rivet. Figure 6 (a) shows that when the anvil continues to press down to 2/3 of the stroke, as grooves 1-4 are filled, significant stress is generated inside these corresponding grooves, reaching a maximum value of 841 MPa. Furthermore, as indicated in Figure 6 (b), the metal of the locking collar exhibits a tendency to continue flowing downwards. Figure 7 (b) shows that upon completion of riveting, the metal completely fills grooves 5-7. Correspondingly, as shown in Figure 7 (a), the stress in the grooves reaches 919 MPa, indicating that the entire connection system has essentially completed metal filling and formed a cooperative load-bearing structure. This verifies the formation mechanism whereby the preload accumulates progressively as the grooves are filled.

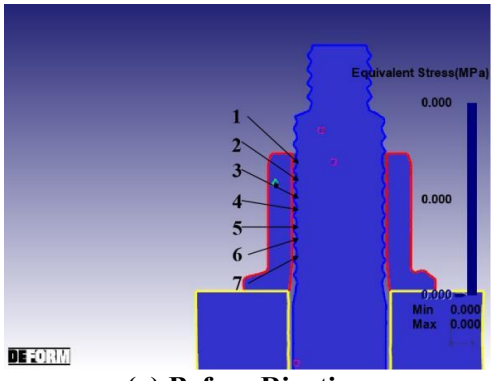

(a) Before Riveting

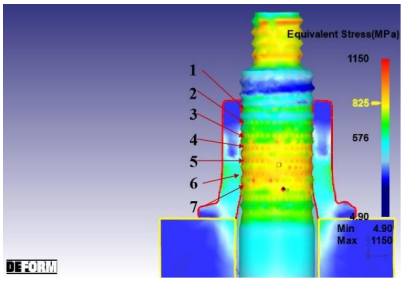

(b) After Riveting

Figure 5. Schematic of Metal Filling Area in the Locking Collar of the Grooved Rivet Assembly

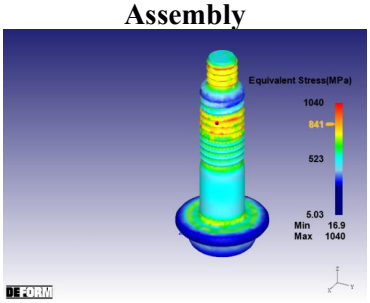

(a) Stress Nephogram of Rivet

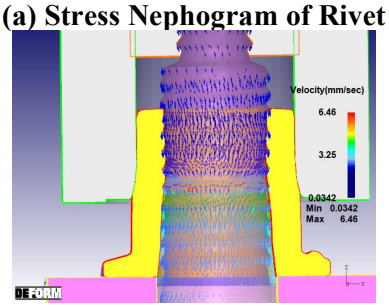

(b) Metal Flow Vector Diagram of Locking Collar

Figure 6. Mechanical Response at 2/3 Riveting Stage

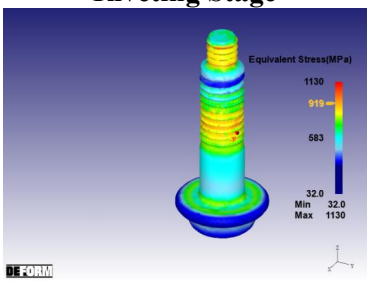

(a) Stress Nephogram of Rivet

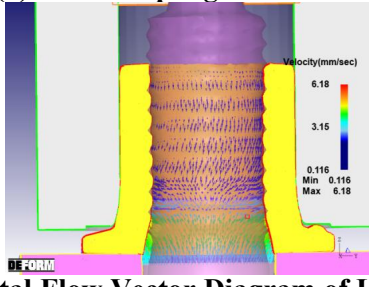

(b) Metal Flow Vector Diagram of Locking Collar

Figure 7. Mechanical Characteristics at Completed Riveting State

4. Experimental Verification and Result Analysis

The finite element simulation results indicate that the preload formation in grooved rivets is a stepwise accumulation process: during riveting, the downward movement of the anvil continuously compresses the locking collar, causing the metal of its inner wall to flow into the rivet grooves under the radial component force. This induces elastic deformation and stress at the corresponding grooves of the rivet shank. This process proceeds stepwise with the anvil displacement until the flange face of the locking collar contacts the anvil, ultimately resulting in the total preload formed by the combined action of all grooves. To verify the accuracy of the aforementioned numerical model and the mechanism of preload generation, this section designs a systematic preload testing experiment.

4.1 Test Scheme

The test system primarily consists of three parts: a preload data acquisition device, specialized riveting tools, and an intelligent pump station with controlled displacement, arranged as shown in Figure 8(a). To precisely study the variation of preload with the riveting progress, the effective riveting length of the locking collar was equally divided into seven stages (L1~L7), as shown in Figure 8(b). During the test, using the top end face of the locking collar as a reference, the intelligent pump station controlled the anvil to sequentially move to these seven preset displacement points. After completing the riveting at each displacement point, the anvil retracted, and the preload value for that stage was recorded by an axial force sensor installed below the locking collar. This segmented riveting method aimed to establish the correspondence curve between displacement and preload, revealing the accumulation mechanism of the preload.

4.2 Test Results and Discussion

A total of 8 valid specimens were prepared for the test (some specimens are shown in Figure 9) and divided into three groups for comparative study:

Group 1 (Specimens 1-3): Employed segmented riveting formation, i.e., riveting was completed in seven steps according to the sequence L1 to L7, recording the preload at each step.

Group 2 (Specimens 4-6): Employed single-step riveting formation, riveting directly to the final displacement L7, measuring the final preload.

Group 3 (Specimens 7-8): Employed two-step riveting formation, first riveted to L1, then directly riveted to L7, measuring the preload at both stages.

(a) Test Equipment Composition

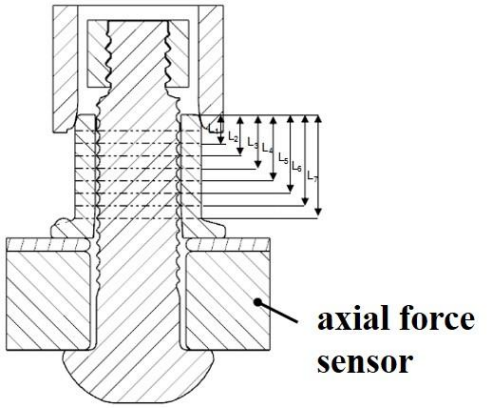

(b) Schematic of Segmented Riveting Test

Figure 8. Schematic Diagram of the Preload Test Setup

Figure 9. Some Test Grooved Rivet Assemblies

The detailed test data for segmented riveting are recorded in Table 2, and its preload-displacement relationship curve is shown in Figure 10. The final results for single-step and two-step riveting are summarized in Table 3 and Table 4, respectively.

Comprehensive analysis of the test data leads to the following conclusions:

Characteristics of the Initial Preload Stage: When the anvil completed the riveting of the first groove (displacement L1), the preload generated by the three segmented riveting specimens was all less than 1 kN (0.5 kN, 0.7 kN, 0.7 kN). This indicates that in the initial stage, the metal of the locking collar only begins to undergo minor flow, and the radial clamping effect on the rivet shank has not yet been effectively established, contributing minimally to the preload.

Significant Preload Generation and Linear Accumulation: Starting from the second displacement stage (L2), the preload increased significantly, reaching approximately 10.2kN, 10.4kN, and 9.8kN for the three specimens, respectively, with a change of about 10kN. From L2 to the final displacement L7, the preload increment per displacement stage averaged about 14kN (e.g., Specimen 1: 13.8kN, 13.9kN, 16.1kN, 15.1kN, 14.6kN, 15.8kN), and a good linear growth relationship was observed between preload and anvil displacement (Figure 10). This result clearly verifies the "multi-stage locking effect" revealed by the finite element analysis: the preload is the result of the stepwise accumulation of radial clamping forces applied to the rivet shank as the collar metal is sequentially extruded into each groove.

Robustness of the Riveting Process: Comparing the final preload from the three riveting processes segmented riveting formation (85.6kN, 86.8kN, 85.3kN), single-step riveting formation (86.2kN, 86.8kN, 85.1kN), and two-step riveting formation (85.3kN, 85.6kN) the deviation in the final preload is within 1kN, showing high consistency. This indicates that the final preload of the Grooved Rivet is primarily determined by the final engagement state between the locking collar and the rivet grooves and is insensitive to the intermediate riveting path. This characteristic is of great significance for on-site construction in wind power applications, ensuring stable and reliable connection preload even under slightly varying installation rhythms.

Table 2. Preload Test Data for Segmented Riveting Formation

Specimen ID	Riveting State	Displacement Stage	Preload (kN)
1	Segmented Riveting	1	0.5
		2	10.2
		3	24
		4	40.1
		5	55.2
		6	69.8
		7	85.6
2	Segmented Riveting	1	0.7
		2	10.4
		3	23.9
		4	40.4
		5	55.3
		6	70.3
		7	86.8
3	Segmented Riveting	1	0.7
		2	9.8
		3	23.5
		4	38.8
		5	54.2
		6	68.7
		7	85.3

Table 3. Final Preload Data for Single-Step Riveting Formation

Specimen ID	Riveting State	Displacement Stage	Preload (kN)
1	Single-Step Riveting	7	86.2
2			86.8
3			85.1

Table 4. Preload Data for Two-Step Riveting Formation

Specimen ID	Riveting State	Displacement Stage	Preload (kN)
1	Two-Step Riveting	1	0.8
		7	85.3
2	Two-Step Riveting	1	0.4
		7	85.6

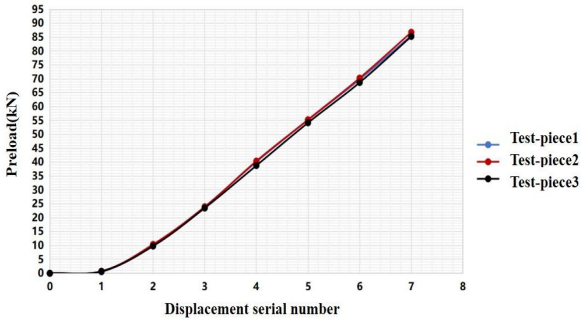

Figure 10. Preload-Displacement Relationship Curve for Segmented Riveting

5. Conclusion

Addressing the urgent demand for high-strength fastening connections in wind power equipment, this study focused on Grooved Rivets. Utilizing a combined approach of finite element numerical simulation and systematic experimental verification, an in-depth investigation was conducted into their preload formation mechanism, the plastic flow behavior of the locking collar, and the connection performance. This revealed the "multi-stage locking" formation mechanism of the preload. This mechanism indicates that the preload in Grooved Rivets is not generated instantaneously but originates from the stepwise accumulation of radial clamping forces produced as the locking collar metal is sequentially and continuously extruded into the individual grooves on the rivet shank under the compression of the anvil during the riveting process. Finite element analysis clearly illustrated the evolution of the metal flow vectors and stress in the locking collar with anvil displacement, demonstrating a significant linear growth relationship between the preload and the anvil displacement.

Furthermore, the robustness of the installation process was confirmed. By comparing the test results of segmented, single-step, and two-step riveting processes, it was found that the deviation in the final preload achieved by the three processes was less than 1 kN, exhibiting high consistency. This indicates that the final connection performance of Grooved Rivets is insensitive to the intermediate riveting path and depends primarily on the final engagement state between the locking collar and the rivet grooves. This characteristic is of great significance for ensuring consistent and reliable on-site construction quality in wind power applications. The study fundamentally elucidates the multi-stage locking principle of preload generation in high-strength Grooved Rivets for wind power, verifies their connection reliability and process robustness, and provides a solid theoretical basis and practical guidance for the widespread application and process optimization of Grooved Rivets in critical industrial fields such as wind power.

Acknowledgments

This project is sourced from the Demonstration Project of Science and Technology Achievements Transfer and Transformation in Sichuan Province (2024ZHCG0129); and the Major Project of CRRC Corporation Limited (2023CKB346).

References

[1] Zhang Tianxiong, Wang Yuanqing, Chen Zhihua, et al. Experimental Study on Mechanical Properties of High-Strength Stainless Steel Short-Tail Grooved Rivets. Engineering Mechanics, 38(S01):8.

[2] Zhang Qin, Zhang Peng, Jia Yunlong, et al. Experimental Study on Grooved Rivets Based on Deform Numerical Simulation. Forging Equipment & Metalforming Technology, 2020, 33(3):130-134.

[3] Li Wenchao, Qian Wei, Yan Qiang, et al. Simulation Study on Interference-Fit Riveting Based on DEFORM-3D. Journal of University of Shanghai for Science and Technology, 2014, 36(5):479-482.

[4] Chen Weijing. Research on Loosening Mechanism and Anti-loosening Technology of Threaded Connections. Scientific and Technological Innovation, 2022, (30):175-179.

[5] Li Jin, Xie Suming, Ma Qiaoyan, et al. Research on Modeling Method for Strength Analysis of Connection Structures Based on Riveting Forming. Mechanical Engineering & Automation, 2025(2).

[6] Zuo Shibin, Jia Yunlong, Zhang Qin, et al. Research on Ultrasonic Testing Method for Clamping Force of Grooved Rivets Based on Acoustoelasticity Principle. 2021.

[7] Li Huixun, Hu Yingchun, Zhang Jianzhong. Study on Simulation of Bolt Preload Using ANSYS. Journal of Shandong University of Science and Technology: Natural Science Edition, 2006, 025(001):57-59.

[8] Zhou Kun, Liu Meihong. Analysis of Calculation and Control Methods for Bolt Preload in Flange Bolt Connections. New Technology & New Process, 2010(8):3.

[9] Qian Jin, Chen Guo, Cun Wenyuan, et al. High-Fidelity Finite Element Simulation and Experimental Verification of Bolt Preload Under Tightening Torque. Journal of Mechanical Strength, 2024, 46(4):809-815.

[10] Huang Jiawei. Orthogonal Experimental Analysis of Bolt Connection Strength. Modeling and Simulation, 2024, 13.

[11] Dai Runda, Yu Hongjie, Fu Changyi, et al. Experimental Study on Corrosion

Resistance and Clamping Force of Grooved Rivet Connection Assemblies in Group Riveting. World Bridges, 2023, 51(2):76-81.
[12]Wang Wen, Luo Yuhang, Li Shihua. Analysis and Research on the Correspondence Between Blade Load and Bolt Preload. China Plant Engineering, 2025(2):138-140.